New Phytologist

Research

A reactive oxygen species Ca^{2+} signalling pathway identified from a chemical screen for modifiers of sugar-activated circadian gene expression

Xiang Li[1], Dongjing Deng[1], Gizem Cataltepe[1,2], Ángela Román[1], Christopher R. Buckley[1], Carolina Cassano Monte-Bello[2], Aleksandra Skirycz[2], Camila Caldana[2] and Michael J. Haydon[1]

[1]School of BioSciences, University of Melbourne, Parkville, Vic. 3010, Australia; [2]Max Planck Institute of Molecular Plant Physiology, 14476 Potsdam, Germany

Author for correspondence:
Michael J. Haydon
Email: m.haydon@unimelb.edu.au

Received: *16 June 2022*
Accepted: *13 July 2022*

New Phytologist (2022) **236:** 1027–1041
doi: 10.1111/nph.18380

Key words: *Arabidopsis thaliana*, calcium, calmodulin, circadian clock, LOPAC (Library of Pharmacologically Active Compounds), reactive oxygen species (ROS), sugar signalling, superoxide.

Summary

- Sugars are essential metabolites for energy and anabolism that can also act as signals to regulate plant physiology and development. Experimental tools to disrupt major sugar signalling pathways are limited. We performed a chemical screen for modifiers of activation of circadian gene expression by sugars to discover pharmacological tools to investigate and manipulate plant sugar signalling.
- Using a library of commercially available bioactive compounds, we identified 75 confident hits that modified the response of a circadian luciferase reporter to sucrose in dark-adapted *Arabidopsis thaliana* seedlings. We validated the transcriptional effect on a subset of the hits and measured their effects on a range of sugar-dependent phenotypes for 13 of these chemicals. Chemicals were identified that appear to influence known and unknown sugar signalling pathways.
- Pentamidine isethionate was identified as a modifier of a sugar-activated Ca^{2+} signal that acts as a calmodulin inhibitor downstream of superoxide in a metabolic signalling pathway affecting circadian rhythms, primary metabolism and plant growth.
- Our data provide a resource of new experimental tools to manipulate plant sugar signalling and identify novel components of these pathways.

Introduction

Cells depend on sugars to generate energy and to build the molecules required for cellular form and function. Sugars can also act as signalling molecules with various roles in regulating growth and development, physiological processes, metabolic feedback, and modulating abiotic or biotic stress responses (Rolland *et al.*, 2006). Plants generate their own sugars from photosynthesis. This dependence on light for energy supply creates specific challenges for plant cells, which must maintain these processes under both predictable and unpredictable fluctuations in the growth environment. This requires multiple sugar signalling pathways to coordinate dynamic supply and demand throughout the plant.

There are four well-recognised sugar signalling pathways in plants. HEXOKINASE 1 (HXK1) is responsible for the first enzymatic step in glycolysis but has glucose signalling functions independent of its enzymatic activity (Moore *et al.*, 2003). G-protein signalling plays a role in extracellular glucose sensing and cell proliferation (Chen *et al.*, 2003; Urano *et al.*, 2012). TARGET OF RAPAMYCIN (TOR) kinase functions in numerous signalling pathways and is activated under carbon (C)-replete conditions (Xiong *et al.*, 2013). By contrast, Snf1 RELATED KINASE 1 (SnRK1) is active under C starvation (Baena-González *et al.*, 2007). SnRK1 activity is inhibited by the signalling sugar trehalose-6-phosphate (T6P) (Zhang *et al.*, 2009), which is very tightly connected to sucrose levels (Figueroa & Lunn, 2016). SnRK1, and perhaps also TOR, can directly affect activity of transcription factors (Xiong *et al.*, 2013; Mair *et al.*, 2015). HXK1 can localize to the nucleus and associate with DNA-binding complexes (Cho *et al.*, 2006).

The critical importance of sugar signalling in plant cells makes genetic analysis of these pathways challenging. Loss-of-function mutants in *TOR* or *T6P SYNTHASE 1* (*TPS1*) are embryo lethal (Eastmond *et al.*, 2002; Menand *et al.*, 2002) and a double mutant in both catalytic subunits of SnRK1 is not viable (Ramon *et al.*, 2019). Therefore, most studies on these pathways have used hypomorphic mutants or inducible transgenic lines (Baena-González *et al.*, 2007; Gómez *et al.*, 2010; Xiong *et al.*, 2013; Belda-Palazón *et al.*, 2020). By contrast, growth effects in mutants in *HXK1* or *REGULATOR OF G-PROTEIN SIGNALLING 1* (*RGS1*) are relatively minor, but both mutants are hyposensitive to growth inhibition by high exogenous sugar (Moore *et al.*, 2003; Chen *et al.*, 2006).

Although there is substantial overlap between the cellular processes controlled by these sugar signalling pathways, particularly

growth and energy metabolism, there are distinct features of their signalling outputs. For example, genetic experiments indicate additive effects of *hxk1-3* and *rgs1-2* mutants (Huang *et al.*, 2015), suggesting functionally distinct pathways. TOR regulates proteostasis, autophagy and cell cycle control by sugars (Burkart & Brandizzi, 2021), whereas SnRK1 controls responses to energy deprivation and regulation of iron homeostasis (Peixoto *et al.*, 2021).

The circadian clock is a gene regulatory network that integrates external and intrinsic signals to coordinate biological rhythms according to daily and seasonal changes in the environment. Photoautotrophic metabolism requires feedback between C availability and the circadian oscillator to optimise plant growth and fitness. Sugars affect circadian rhythms in Arabidopsis in several ways. C status contributes to entrainment, the process of setting the phase of the circadian clock (Haydon *et al.*, 2013), and measurement of photoperiod (Liu *et al.*, 2021). Reduced photosynthesis lengthens the circadian period, which can be suppressed by supplying sugar (Haydon *et al.*, 2013). Period adjustment by sugars requires T6P-SnRK1 signalling affecting transcription of *PSEUDO RESPONSE REGULATOR 7* (*PRR7*) (Frank *et al.*, 2018). Sugars can also affect the amplitude of specific oscillator components. One mechanism occurs by posttranscriptional control of GIGANTEA (GI) and requires F-box protein ZEITLUPE (ZTL) (Haydon *et al.*, 2017).

Circadian rhythms rapidly dampen in seedlings released into continuous darkness without supplied sugar. Application of sucrose to dark-adapted seedlings can reinitiate circadian rhythms and the phase is set according to the time of sugar application (Dalchau *et al.*, 2011). This transcriptional response to sugar does not require GI and the signalling processes are not known. This simple assay provides a sensitive technique to define sugar responses in the absence of light signals. We recently used transcriptome analysis of this response to reveal a role for superoxide, a reactive oxygen species (ROS), in promoting circadian gene expression and growth by sugar (Román *et al.*, 2021). To further understand the signalling underlying this transcriptional response to sugar, we screened the Library of Pharmacologically Active Compounds (LOPAC; Sigma-Aldrich) for chemicals that modify the response of a circadian reporter to sucrose in dark-adapted seedlings. From a list of 75 confident hit compounds, we selected 15 compounds to further characterize their effects on sugar-dependent processes. We focus on two compounds that inhibit a sugar-activated ROS-Ca^{2+} signalling pathway that affects circadian rhythms, primary metabolism and plant growth. Our data provide a resource of pharmacological tools to manipulate sugar signalling in plants and has revealed opportunities to define new components of metabolic signalling.

Materials and Methods

Plant materials

Transgenic reporter lines in *Arabidopsis thaliana* for *COLD, CIRCADIAN RHYTHM AND RNA BINDING 2* (*CCR2*) promoter: *LUCIFERASE* (*LUC*) (Doyle *et al.*, 2002), *DARK INDUCIBLE 6* (*DIN6*)*p:LUC* (Frank *et al.*, 2018), *CaMV 35Sp:AEQUORIN* (*AEQ*) (Dalchau *et al.*, 2010), *CIRCADIAN CLOCK ASSOCIATED 1* (*CCA1*)*p:LUC* (CS9382), *PRR7p:LUC* (Haydon *et al.*, 2013) and *TIMING OF CAB 1* (*TOC1*)*p:LUC* (Nakamichi *et al.*, 2005) are in Col-0, while *35Sp:LUC* (CS9966) is in Ws-2. The *glucose insensitive 2* (*gin2-1*), *abscisic acid 2* (*aba2-1*), and *constitutive triple response 1* (*ctr1-12*) with a *CCA1p:LUC* transgene have been described (Haydon *et al.*, 2013). *CCA1p:LUC* was introduced by crossing into *g protein alpha subunit 1* (*gpa1-4*) (Jones *et al.*, 2003), *gtp binding protein 1* (*agb1-4*) (Ullah *et al.*, 2003) and *rgs1-2* (Chen *et al.*, 2003). The *g-protein gamma subunit 1* (*agg1-1*) *agg2-1 agg3-3* triple mutant (Thung *et al.*, 2012) and *casein kinase a 1* (*cka1-1*) *cka2-1 cka3-1* triple mutant (Wang *et al.*, 2014) were generated previously.

Growth conditions

For sterile culture, seeds were surface sterilised (30% (v/v) bleach, 0.02% (v/v) Triton X-100), washed three times in sterile water and sown on modified Hoagland media (HM) (Haydon *et al.*, 2012) or half-strength Murashige & Skoog media (½MS) (Sigma-Aldrich), 3 mM MES-KOH (pH 5.7), solidified with 0.8% (w/v) agar Type M (Sigma-Aldrich). Seeds were chilled for 2 d at 4°C and grown under 12 h light (80–100 μmol m^{-2} s^{-1}) : 12 h dark at constant 20°C (L : D).

Chemical screen

Seven-day-old *CCR2p:LUC* seedlings grown under L : D (see 'Growth conditions' in the Materials and Methods section) on HM were wrapped in aluminium foil at dusk. Under dim green light, individual 10-d-old seedlings were transferred in the afternoon to 96-well white LUMITRAC plates (Greiner, Stonehouse, UK) containing 250 μl HM with 0.1% DMSO or 25 μM LOPAC chemical (Sigma-Aldrich) and dosed with 1 mM D-luciferin, K^+ salt (Cayman Chemical, Ann Arbor, MI, USA). Eighty LOPAC chemicals were included in each plate, plus positive and negative controls. Each plate was prepared in triplicate. After 84 h in darkness (subjective dawn), 25 μl of 10% (w/v) sucrose or mannitol was added and luciferase was measured at 1 h intervals for 24 h in the dark using orbital scan mode in a LUMIstar Omega plate reader fitted with a Microplate stacker (BMG Labtech, Aylesbury, UK). HiTSeekR (List *et al.*, 2016) was used to identify compounds that significantly altered peak luminescence at 12 h after sucrose application after removing 47 data series from the total 4224 deemed as false negatives. The raw data were $\log_2$ transformed and normalized with the robust *z*-score method for general signal difference correction and inter-plate comparison before calculation of strictly standardized mean difference (SSMD) values.

Luciferase assays

For sugar response assays, 7-d-old seedlings grown under L : D on ½MS were wrapped in aluminium foil at dusk. After 72 h, seedlings were transferred to ½MS containing chemicals in 96-well LUMITRAC plates under dim green light and sugars were

added 12 h later at subjective dawn. Also, 1 mM D-luciferin was applied at least 12 h before commencing luminescence measurements using the orbital scan mode in a LUMIstar Omega plate reader with Microplate stacker (BMG Labtech). Circadian rhythms were measured in 8-d-old *CCA1p:LUC*, *PRR7p:LUC*, *CCR2p:LUC* and *TOC1p:LUC* seedlings grown on ½MS under L : D and transferred at Zeitgeber Time 6 (ZT6) to black 96-well plates containing media with DMSO or chemical the day before imaging luminescence with a Retiga Lumo CCD camera (Teledyne Photometrics, Tucson, AZ, USA) in continuous light (40 μmol m^{-2} s^{-1}) or continuous low light (< 10 μmol m^{-2} s^{-1}) provided by red (640 nm) and blue (470 nm) LED lights.

Quantitative RT-PCR

Total RNA was extracted from *c.* 30 mg snap frozen tissue with ISOLATE II RNA Plant Kit (Meridian Bioscience, Cincinnati, OH, USA). cDNA was prepared from 0.5 μg DNase-treated RNA in 10 μl reactions of a Tetro cDNA synthesis kit (Meridian Bioscience) using oligo(d)T primer. PCRs (10 μl) were performed in technical duplicate with SensiFAST SYBR No-ROX (Meridian Bioscience) with 4 ng cDNA and 300 nM primers (Supporting Information Table S1) on a CFX96 Real-time PCR System (Bio-Rad). Mean PCR efficiencies were calculated for each primer pair with LinRegPCR (Ruijter *et al.*, 2009) and used to calculate gene expression levels ($PCR\_efficiency^{-Ct}$). *UBQ10* was chosen as the reference gene because it was stable in previous RNA-sequencing (RNA-seq) experiments in equivalent conditions (Román *et al.*, 2021).

Growth assays

Germination was measured in nonchilled, surface-sterilised Col-0 seeds sown onto ½MS with DMSO or chemical and mannitol or sucrose at ZT0 and immediately placed under L : D. Germination was scored as visible radicle emergence from the seed coat using a stereomicroscope at two or three timepoints per day for 4 d. For hypocotyl and root length measurements, Col-0 was grown under L : D on ½MS for 2 d and transferred to media containing DMSO or chemical with 30 mM mannitol or sucrose at ZT0, wrapped in aluminium foil and grown on vertical plates for 5 d. Hypocotyl and root lengths were measured from photographs with ImageJ (NIH, Bethesda, MD, USA).

Pigment quantification

Chlorophyll was extracted from 12 7-d-old seedlings in 250 μl methanol and quantified by absorbance spectrophotometry (Porra, 1989). Anthocyanin was extracted from five 9-d-old seedlings in 250 μl methanol : 1% (v/v) HCl and quantified by absorbance spectrophotometry (Chen *et al.*, 2019).

Phenotype clustering

Principal component analysis (PCA) of 11 mean phenotypic variables for each chemical was performed. The data were then clustered using a *k*-means approach. To determine the most appropriate value of *k* for clustering, the total within-cluster sum-of-squares (WCSS) was calculated and plotted for all possible values of *k* (1–13). The 'elbow' of this plot (where a further increase in *k* does not substantially reduce WCSS) was selected as the value of *k*. Both PCA and *k*-means clustering analyses were performed using the stats package in R (R Core Team, 2021).

ROS measurements

L-012 luminescence for extracellular ROS detection and nitroblue tetrazolium (NBT) staining for superoxide detection were performed in dark-adapted seedlings in liquid ½MS as described (Román *et al.*, 2021).

Sugar quantification

Samples were frozen in liquid N and stored at −80°C. Soluble sugars were extracted in 80% (v/v) ethanol and measured with a sucrose/glucose/fructose calorimetric assay kit (Megazyme, Bray, Ireland) using modified reaction volumes in 96-well plates.

Aequorin experiments

For chemical response assays, *c.* 10 8-d-old *35Sp:AEQ* seedlings grown under L : D on ½MS were transferred before dusk to 100 μl 20 μM coelenterazine (Cayman Chemical) in 96-well LUMITRAC plates (Greiner). When applicable, 50 μl pretreatments for the indicated final concentration were added 30–60 min previously in dim green light. Luminescence was measured at 1 s intervals in the dark from subjective dawn using the orbital scan mode in a LUMIstar Omega plate reader (BMG Labtech) and 50 μl of DMSO or chemicals were added with an injector at 30 s for the indicated final concentration. After 270 s, 150 μl discharge solution (1 M $CaCl_2$, 10% (v/v) ethanol) was injected and cytosolic Ca^{2+} concentration was calculated (Fricker *et al.*, 1999). For sugar response assays, *c.* 10 7-d-old *35Sp:AEQ* seedlings grown under L : D were transferred to 100 μl liquid ½MS with 20 μM coelenterazine at dusk in 96-well LUMITRAC plates (Greiner) and wrapped in aluminium foil. After 84 h (subjective dawn), 50 μl ½MS containing DMSO or chemicals were added in dim green light for a final concentration of 5 μM diphenyleneiodinium (DPI) or 25 μM pentamidine isethionate (PI) and luminescence was measured at 2 min intervals in orbital scan mode in a LUMIstar Omega plate reader (BMG Labtech). After 1 h, 75 μl sucrose or mannitol was added in dim green light for a final concentration of 30 mM with DMSO, 5 μM DPI or 25 μM PI and luminescence was measured at 2 min intervals for 6 h.

RNA-sequencing

Fourteen-day-old Col-0 seedlings grown on ½MS under L : D were transferred to media containing DMSO, 10 μM DPI, 25 μM PI, 12.5 μM AEG3482 or 2 μM Tyrphostin AG879 at ZT24, before lights on. Untreated control seedlings were collected at the time of transfer and treated seedlings were collected

at ZT2 and snap frozen in liquid N. Total RNA was extracted from biological triplicates with an Isolate II RNA Plant kit (Meridian Bioscience) and quantified and qualified by using an Agilent 2100 Bioanalyzer, NanoDrop (ThermoFisher, Waltham, MA, USA) and 1% agarose gel. Total RNA (1 μg) with RIN value above 7 was used for library preparation by Genewiz (South Plainfield, NJ, USA) using a NEBNext Ultra™ RNA Library Prep Kit for Illumina and NEBNext Poly(A) mRNA Magnetic Isolation Module (NEB, Ipswich, MA, USA). Size selection of adaptor-ligated DNA was then performed using AxyPrep Mag PCR Clean-up (Axygen, Union City, CA, USA), and fragments of *c.* 360 bp (with approximate insert size of 300 bp) were recovered. Each sample was then amplified by PCR for 11 cycles using P5 and P7 primers. The PCR products were cleaned up using AxyPrep Mag PCR Clean-up (Axygen), validated using an Agilent 2100 Bioanalyzer, and quantified on a Qubit 2.0 fluorometer (Invitrogen). Libraries with different indices were multiplexed and loaded on an Illumina HiSeq instrument and sequenced using a 2 × 150 bp paired-end (PE) configuration; image analysis and base calling were conducted by the HiSeq Control Software (HCS) + OLB + GAPipeline-1.6 (Illumina, San Diego, CA, USA) on the HiSeq instrument. All libraries had > 20 million raw reads with Q30 and Q20 > 95% and > 98%, respectively.

SOAPnuke v.2.1.0 (Chen *et al.*, 2018) was used to remove adapter sequences and low-quality reads from the sequencing data. To identify all the transcripts, we used Hisat2 v.2.2.1 (Kim *et al.*, 2015) to align the sequencing reads to the *A. thaliana* Col-0 genome (TAIR10) and Rsem v.1.2.22 (Li & Dewey, 2011) to quantify the gene expression level of each replicate. Differential expression analysis was performed by NOIseq v.2.37.0 (Tarazona *et al.*, 2015). Differentially expressed genes (DEGs) were defined based on $\log_2$ change > 0.6 and DE probability > 80%.

Metabolomics

Fourteen-day-old Col-0 seedlings grown hydroponically were transferred to liquid ½MS containing DMSO, 10 μM DPI, 25 μM PI, 12.5 μM AEG3482 or 2 μM Tyrphostin AG879 at ZT23. Tissue was collected for five biological replicates for untreated seedlings at ZT23 and treated seedlings at ZT24 (lights off), ZT1.5, ZT4, ZT8, ZT10.5, ZT12 (lights on), ZT22.5 and ZT24 (lights off) and snap frozen in liquid N. Fifty milligrams of ground tissue was used for MTBE : methanol : water, 3 : 1 : 1 (v/v) extraction (Giavalisco *et al.*, 2011). Then, 150 μl of the organic phase was dried and derivatized (Roessner *et al.*, 2001). One microlitre of the derivatized samples was analysed on a Combi-PAL autosampler (Agilent Technologies, Santa Clara, CA, USA) coupled to an Agilent 7890 gas chromatograph coupled to a Leco Pegasus 2 time-of-flight mass spectrometer (Leco, St Joseph, MI, USA) (Weckwerth *et al.*, 2004). Chromatograms were exported from LECO ChromaTOF software (v.3.25) to R software. Peak detection, retention time alignment and library matching were performed using the targetsearch R-package (Cuadros-Inostroza *et al.*, 2009).

Metabolites were quantified by the peak intensity of a selective mass. Metabolite intensities were normalized by dividing the fresh weight, followed by the sum of total ion count as described previously (Giavalisco *et al.*, 2011; Huege *et al.*, 2011). PCA was performed using the pcaMethods Bioconductor package (Stacklies *et al.*, 2007). The significances of metabolites were tested by a *t*-test.

Results

We exploited the reinitiation of circadian gene expression by sugar in dark-adapted seedlings to evaluate transcriptional sugar responses in Arabidopsis. Using a luciferase reporter system, this provides a sensitive, high-throughput assay to measure plant sugar responses in the absence of light. Topical application of 30 mM sucrose to dark-adapted seedlings is sufficient for a robust response of a circadian luciferase reporter *CCR2p:LUC* (Fig. 1a) and generates similar sugar concentrations to seedlings grown in the light (Fig. 1b). Sucrose is the most abundant and mobile soluble sugar in plant tissues, although similar reporter activity is also elicited by glucose, fructose and maltose (Fig. 1c). By contrast, Mg-ATP could not elicit an increase in *CCR2p:LUC* activity (Fig. S1).

Numerous sugar-insensitive mutants have been identified in Arabidopsis that are resistant to growth inhibition by high concentrations of sugars in the media. We tested the transcriptional responses to sucrose in a collection of these mutants using our assay and observed similar responses to wild-type seedlings (Fig. 1d–f). Notably, these included mutants in *HXK1* and G-protein signalling, suggesting these sugar signalling pathways are not required for sugars to reinitiate circadian rhythms in dark-adapted seedlings.

To discover new components involved in plant sugar signalling, we performed a high-throughput screen for chemicals that modify the transcriptional response to sucrose. Dark-adapted *CCR2p:LUC* transgenic seedlings were treated with sucrose in the presence of 25 μM of each of 1280 chemicals from LOPAC (Sigma-Aldrich). This collection of commercially available chemicals have defined targets in mammalian cells, and mostly target signalling proteins such as receptors, kinases and ion channels. We used HiTSeekR (List *et al.*, 2016) to calculate SSMD values. A cut-off of ±1 identified 146 chemicals that significantly modified the peak reporter activity (Table S2). To generate a higher confidence list of candidates, we used a stricter SSMD cut-off of ±1.28, which provided a list of 65 inhibitors and 10 enhancers of the reporter response to sucrose (Table 1).

Greater than 10% of compounds present in chemical libraries are reported to exhibit inhibition of luciferase activity (Thorne *et al.*, 2012). We rescreened 104 chemicals from LOPAC for their effect on luciferase activity at 25 μM using *35Sp:LUC* seedlings (Fig. S2). We identified two compounds that significantly enhanced luciferase luminescence and 11 compounds that significantly inhibited luminescence, indicating these might be false-positives identified in the primary screen.

We selected 15 chemicals (Fig. S3) for further analyses including DPI, which we previously showed inhibits the transcriptional sugar response (Román *et al.*, 2021), 6-methyl-2-(phenylethynyl) pyridine (MPEP), which strongly inhibited *35Sp:LUC* luciferase (Fig. S1), and AZD8055, a specific inhibitor of TOR (Montané

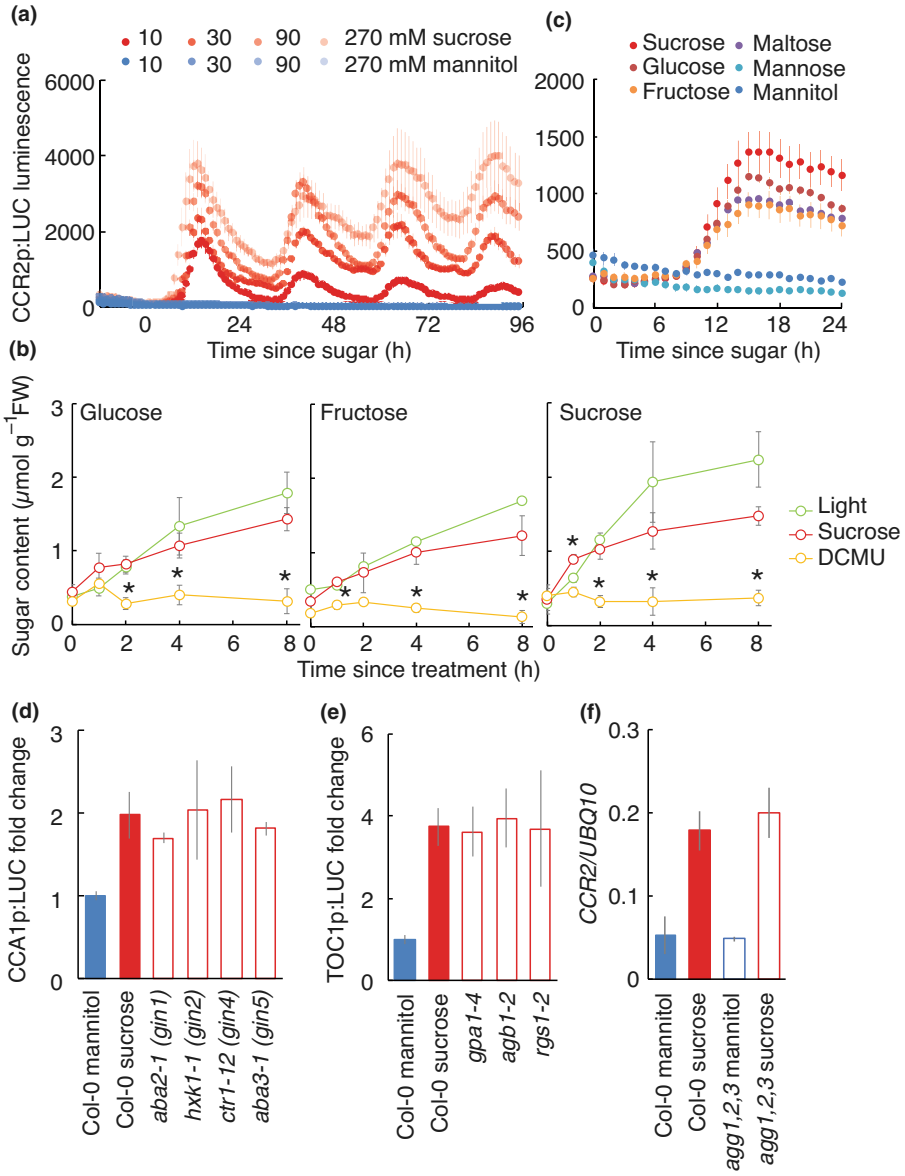

Fig. 1 A sugar response assay in Arabidopsis seedlings. (a) Luciferase luminescence in dark-adapted *CCR2p:LUC* seedlings treated with the indicated concentration of sucrose or mannitol (means ± SEM, $n = 6$). (b) Sugar content in dark-adapted seedlings treated with 30 mM sucrose or transferred to the light with or without 3-(3,4-dichlorophenyl)-1,1-dimethylurea (DCMU) (means ± SD, $n = 4$; *, $P < 0.05$ compared to Light, Bonferroni-corrected *t*-test). (c) Luciferase luminescence in dark-adapted *CCR2p:LUC* seedlings treated with 30 mM sugars (means ± SEM, $n = 8$). (d, e) Fold change of peak luciferase reporter luminescence in dark-adapted wild-type (Col-0) or mutant seedlings treated with mannitol (blue) or sucrose (red) compared to luminescence before treatment (means ± SD, $n = 4$). (f) *CCR2* transcript level, normalized to *UBQ10*, in dark-adapted wild-type (Col-0) or *agg1 agg2 agg3* mutant seedlings 12 h after treatment with mannitol (blue) or sucrose (red) (means ± SD, $n = 3$). (d–f) No significant differences were detected between genotypes ($P > 0.05$, Bonferroni-corrected *t*-tests).

& Menand, 2013), which is not in LOPAC but has been reported to affect circadian sugar responses in Arabidopsis (Zhang *et al.*, 2019). We generated dose–response curves for these 15 chemicals based on inhibition of *CCR2p:LUC* luminescence in dark-adapted seedlings treated with sucrose to determine a minimum effective concentration at which > 80% inhibition is achieved (Figs 2, S4). Although the primary screen was performed with 25 μM, effective concentrations ranged from 2 to 50 μM for these chemicals. By contrast, the maximum inhibition of the luciferase reporter achieved for the TOR inhibitor AZD8055 was only *c.* 50%.

To validate the efficacy of these compounds on the transcriptional response to sugar, we again measured luciferase luminescence in *35Sp:LUC* seedlings at the minimum effective concentration determined from the dose curves (Fig. 3a) and measured *CCR2* transcript in dark-adapted seedlings treated with sucrose using quantitative reverse transcriptase (qRT)-PCR (Fig. 3b). This confirmed that all chemicals inhibited the upregulation of *CCR2* transcript by sucrose to some extent, except for two metabotropic glutamate receptor (mGluR5) inhibitors MPEP and SIB1893, which also significantly reduced luciferase luminescence in *35Sp:LUC* seedlings. We therefore excluded these two chemicals from further experiments. We also observed that 50 μM roscovitine increased 35Sp:LUC luminescence, despite inhibiting response of *CCR2p:LUC* and *CCR2* transcript to sucrose.

One of the validated chemicals, tetrabromobenzotriazole (TBB), is a mammalian casein kinase 2 inhibitor. CK2 is a regulator of the circadian clock and another CK2 inhibitor, dichlorobenzimidazole ribofuranoside (DRB), has been shown to lengthen circadian period in Arabidopsis (Portolés & Más, 2010). We tested whether DRB inhibits the response of *CCR2p:LUC* to sucrose in dark-adapted seedlings and found no effect at the concentrations tested (Fig. S5a). Similarly, we could not detect a

Table 1 Chemical modifiers of *CCR2p:LUC* response to sucrose in Arabidopsis.

Chemical name	PubChem_CID	*rz* score	SSMD	Primary mammalian target
Tyrphostin AG 879	135419190	−13.88	−5.87	TrkA, tyrosine kinase
3,3′-Difluorobenzaldazine (DFB)	006604893	−3.99	−5.13	mGluR5, metabotropic glutamate receptor
6-Methyl-2-(phenylethynyl) pyridine hydrochloride (MPEP)*,†	009794588	−6.58	−4.88	mGluR5, metabotropic glutamate receptor
5-Nitro-2-(3-phenylpropylamino) benzoic acid (NPPB)	000004549	−1.80	−4.84	Cl^- channel
1,9-Pyrazalolanthrone (SP600125)	000008515	−3.81	−4.83	c-Jun N-terminal kinase (c-JNK), MAP kinase
2-Methyl-6-(2-phenylethenyl)pyridine (SIB 1893)	005311432	−6.32	−4.60	mGluR5, metabotropic glutamate receptor
MTEP hydrochloride	045073467	−5.07	−3.78	mGluR5, metabotropic glutamate receptor
L2-b	039247144	−5.59	−3.74	Amyloid-β
Riluzole	000005070	−4.10	−3.56	Na^+ channel
AEG 3482	000698112	−4.86	−3.39	Heat shock protein 90 (HSP90)
Niclosamide	000004477	−2.70	−3.30	Oxidative phosphorylation
CGP-7930	005024764	−4.03	−3.26	GABA-B receptor, GPCR
Tyrphostin 51	005328807	−2.26	−3.22	EGF receptor, tyrosine kinase
4,5,6,7-Tetrabromobenzotriazole (TBB)	000001694	−9.98	−3.19	Casein kinase 2 (CK2)
Fenobam	000162834	−1.32	−3.12	mGluR5, metabotropic glutamate receptor
DMH4	005329447	−3.69	−3.00	VEGF receptor, tyrosine kinase
Bay 11-7082	005353431	−2.07	−2.81	Nuclear factor-kappa B (NF-κB), transcription factor
1-Phenyl-3-(2-thiazolyl)-2-thiourea†	000719408	−5.59	−2.81	Dopamine beta-hydroxylase
BF-170 hydrochloride*	000297284	−4.93	−2.78	Tau
Diphenyleneiodonium chloride (DPI)	002733504	−11.81	−2.65	Nitric oxide synthase (NOS)
CBIQ	011401613	−2.18	−2.65	CFTR Cl^- channel
PD 98,059*	000004713	−4.29	−2.58	MAP kinase kinase (MAPKK)
Oltipraz metabolite M2	000128585	−4.38	−2.57	Liver X receptor α (LXR-α)
Nocodazole*	000004122	−2.06	−2.52	Beta-tubulin
L-165,041	006603901	−3.39	−2.44	Peroxisome proliferator-activated receptor (PPAR)
Amlexanox*,†	000002161	−5.63	−2.37	TANK-binding kinase 1, Ser/Thr kinase
2,3-Dimethoxy-1,4-naphthoquinone (DMNQ)	000003136	−6.91	−2.32	Redox cycling agent
Rhodblock 6	006466029	−3.49	−2.21	Rho kinase, Ser/Thr kinase
DCEBIO	000656765	−1.48	−2.20	K^+ and Cl^- channel
3,4,-Methylenedioxy-β-nitrostyrene (MNS)	000672296	−6.11	−2.18	Src and Syk tyrosine kinase
U0126	003006531	−2.01	−2.17	MAP kinase kinase (MAPKK)
Gossypol	000003503	−0.76	−2.13	Platelet activating factor (PAF)
SB-366791	000667594	−2.73	−2.12	TRPV1 cation channel
L-α-Methyldopa	000038853	−0.55	−2.02	L-Aromatic amino acid decarboxylase inhibitor
SMER28	001560402	−1.66	−1.97	Autophagy
SIB 1757	006849066	−3.69	−1.92	mGluR5, metabotropic glutamate receptor
Sanguinarine chloride	000068635	−3.94	−1.87	Protein phosphatase 2C (PP2C)
Nimesulide	000004495	−3.16	−1.81	Cyclooxygenase-2 (COX-2)
Rabeprazole sodium	014720269	−1.62	−1.75	H^+/K^+ ATPase
ONO-RS-082*	006438389	−0.90	−1.61	Phospholipase A2
SU 4312	006450842	−3.30	−1.56	VEGF receptor, tyrosine kinase
Diethylenetriaminepentaacetic acid (DTPA)	000003053	−1.02	−1.55	Metal chelator
JW55	002946601	−2.37	−1.54	Poly (ADP-ribose) polymerase (PARP)
GBR-12909 dihydrochloride	000104920	−3.43	−1.52	Dopamine reuptake
AC-93253 iodide*	016078948	−5.55	−1.52	Retinoic acid receptor (RARalpha)
Ro 61-8048	005282337	−2.16	−1.51	Kynurenine 3 monooxygenase (KMO)
Flunarizine dihydrochloride	005282407	−1.85	−1.50	Ca^{2+}/Na^+ channel
BIO	005287844	−0.95	−1.49	Glycogen synthase kinase 3 (GSK-3)
Pentamidine isethionate	000008813	−1.48	−1.49	NMDA glutamate receptor, Ca^{2+} channel
ZM 39923 hydrochloride	000176406	−3.70	−1.46	Janus kinase 3 (JNK-3), tyrosine kinase
Diclofenac sodium	005018304	−1.71	−1.44	Cyclooxygenase (COX)
Phosphonoacetic acid	000000546	−0.88	−1.42	DNA polymerase
Emodin	000003220	−1.57	−1.37	Casein kinase 2 (CK2)
PF 3845 hydrate	025154867	−2.32	−1.37	Fatty acid amide hydrolase (FAAH)
Naltrindole hydrochloride	016219715	−0.37	−1.35	Delta opioid receptor, GPCR
Tranylcypromine hydrochloride	002723716	−0.71	−1.34	Monoamine oxidase
KRM-III	000736689	−2.41	−1.34	T cell antigen receptor (TCR)
3,4-Dichloroisocoumarin	000001609	−2.23	−1.38	Serine protease
Reactive Blue 2	000108094	−1.54	−1.32	P2Y, purigenic GPCR
TBBz	005149739	−1.36	−1.31	Casein kinase 2 (CK2)
Nemadipine-A	002856102	−0.61	−1.31	L-type Ca^{2+} channel

Table 1 (Continued)

Chemical name	PubChem_CID	*rz* score	SSMD	Primary mammalian target
Danazol	000028417	−1.82	−1.31	Androgen receptor, transcription factor
Nitisinone	000115355	−1.34	−1.30	4-Hydroxyphenylpyruvate dioxygenase (HPPD)
Leflunomide	000003899	−1.35	−1.28	Dihydroorotate dehydrogenase
6(5H)-Phenanthridinone	000001853	−1.82	−1.28	Poly (ADP-ribose) polymerase (PARP)
5α-Pregnan-3α-ol-20-one	000092786	1.24	1.31	GABA-A receptor, ion channel
A3 hydrochloride	009861903	1.03	1.34	Casein kinase (CK)
Candesartan cilexetil	000002540	0.99	1.39	Angiotensin II receptor (ATR), GPCR
S-Methyl-L-thiocitrulline acetate	011957614	0.99	1.41	Nitric oxide synthase (NOS)
Methoxamine hydrochloride	000006081	0.81	1.41	α1 adrenergic receptor, GPCR
Piribedil maleate	011957664	0.90	1.48	Dopamine receptor, GPCR
Phentolamine mesylate	000091430	1.40	1.62	α adrenergic receptor, GPCR
1-Methylhistamine dihydrochloride	011957601	0.86	1.64	Histamine metabolite
Isonipecotic acid	000003773	2.09	1.73	GABA-A receptor, ion channel
GANT61	000421610	1.07	1.75	Zinc finger protein GLI, transcription factor

*Inhibited 35Sp:LUC.
†Luciferase inhibitor from Thorne *et al*. (2012).

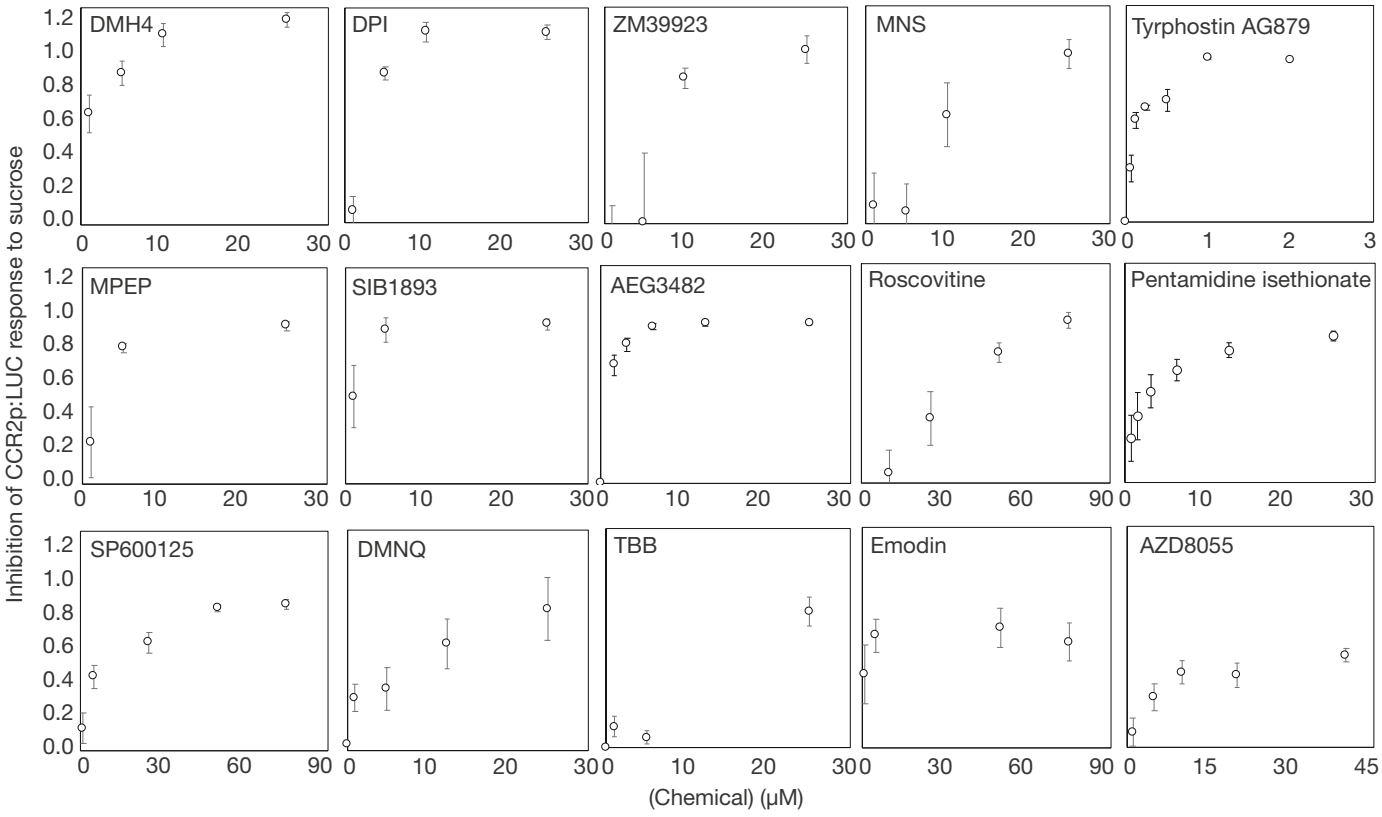

Fig. 2 Dose–response of the transcriptional response to sucrose for 15 chemicals. Inhibition of peak luciferase luminescence in dark-adapted *CCR2p:LUC* Arabidopsis seedlings after treatment with 30 mM sucrose in the presence of the indicated concentration of a chemical compared to DMSO-treated controls (means ± SD, $n = 6$–12).

difference in *CCR2* transcript in *cka1-1 cka2-1 cka3-1* mutants compared to the wild-type using qRT-PCR in the same assay (Fig. S5b). These data suggest that it is unlikely that TBB inhibits the transcriptional response to sucrose by targeting CK2 in Arabidopsis seedlings.

To build a picture of the broader influence of these selected chemicals on sugar-related processes, we tested their effects on a range of easily measurable phenotypes. Using the predetermined minimum effective concentration for each chemical, we tested effects in the presence or absence of sucrose on germination of dormant seeds (Fig. S6), seedling biomass, Chl content, hypocotyl length, root growth and anthocyanin content (Fig. S7). We observed a range of effects of each chemical on these phenotypes but detected similar patterns for multiple chemicals that might

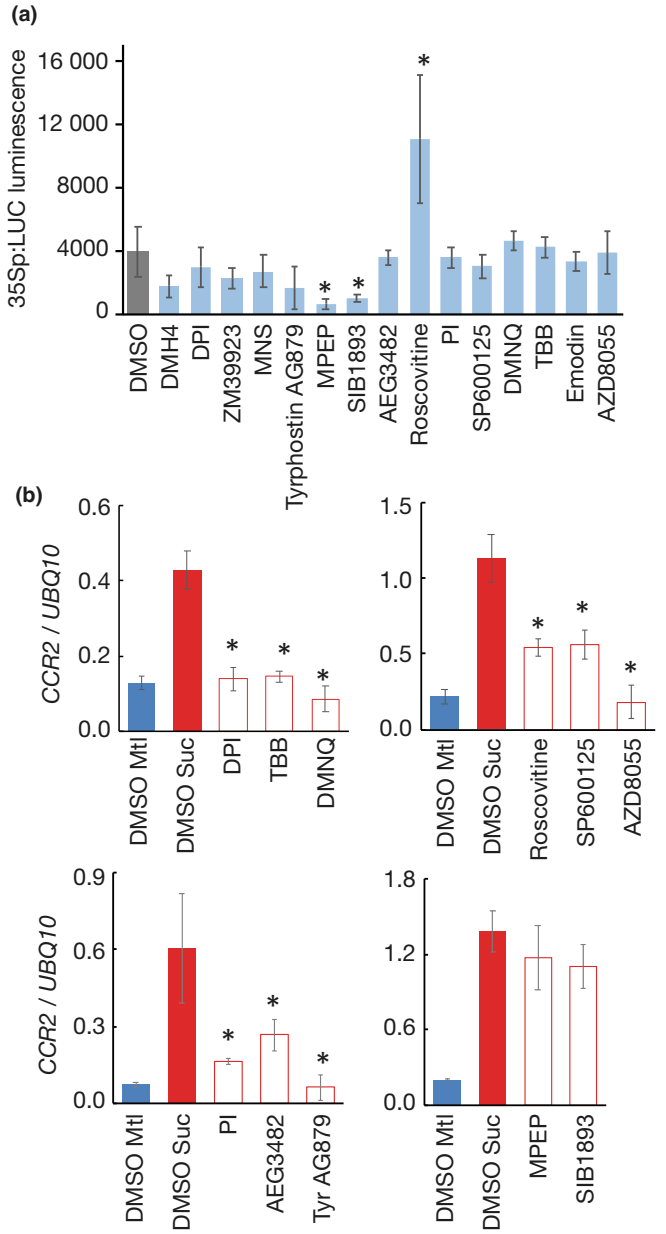

Fig. 3 Validation of transcriptional effect of LOPAC chemicals. (a) Luciferase luminescence in *35Sp:LUC* Arabidopsis seedlings, 16 h after transfer to media containing the minimum effective concentration of each chemical (means ± SD, $n = 8$; *, $P > 0.05$, Bonferroni-corrected *t*-test). (b) *CCR2* transcript level, relative to *UBQ10*, in dark-adapted Arabidopsis Col-0 seedlings 12 h after treatment with 30 mM mannitol (blue), 30 mM sucrose (red) or 30 mM sucrose in the presence of the minimum effective concentration of the chemical (white) (means ± SD, $n = 4$; *, $P > 0.05$, Bonferroni-corrected *t*-test).

indicate common signalling pathways. To summarise these patterns, we plotted normalised effects of phenotypes on radar charts and ranked the chemicals by the sum of effects (Fig. 4a). Based on these radar charts, we noticed similar phenotypic patterns for DPI and PI; emodin and SP600125; and Tyrphostin AG879, DMH4 and ZM39923. PCA of the phenotypic data followed by *k*-means clustering revealed similar patterns (Fig. 4b). Thus, the clusters might indicate these chemicals affect proteins or signalling pathways with closely related functions.

We next tested phenotypic interactions between a selected number of chemicals. We hypothesised that chemicals that affect the same signalling pathway should be nonadditive, whereas chemicals that affect distinct pathways might show a phenotypic interaction in combination. We germinated seeds on media containing chemicals alone or in combination at a 50% inhibitory concentration (Fig. 2) and measured biomass of 7-d-old seedlings (Fig. S8). DPI and PI in combination did not inhibit seedling growth compared to DPI alone, suggesting they affect the same pathway, consistent with the similar pattern for these chemicals in the radar charts. By contrast, Tyrphostin AG879 significantly suppressed the growth inhibition by DPI, indicating these chemicals might act on distinct pathways.

To measure the broader effects of these four chemicals on gene expression, we treated seedlings with each chemical at dawn and performed RNA-seq in seedlings after 2 h to capture short-term transcriptional effects at the beginning of the photoperiod. We identified 1899 DEGs between ZT0 and ZT2 (DMSO), but we detected between one and 16 DEGs between DMSO and any chemical (Table S3; Fig. S9a,b). This might be because the effect of inhibiting sugar signalling at dawn is diminished in the presence of abrupt light signalling. It is also possible that since superoxide-regulated genes are biased towards dusk (Román *et al.*, 2021), the short-term effect of DPI is minimal around dawn. Nevertheless, more than two-thirds of DEGs in chemical-treated seedlings vs controls have been previously reported as sugar-regulated genes (Fig. S9b) (Xiong *et al.*, 2013; Ganpudi *et al.*, 2019; Peixoto *et al.*, 2021; Román *et al.*, 2021). This suggests that these four chemicals all have a major influence on sugar signalling or metabolism. *PATHOGEN AND CIRCADIAN CONTROLLED 1* (*PCC1*), a light-induced flowering time regulator (Segarra *et al.*, 2010), was identified as a DEG for DPI, PI and AEG3482, but not Tyrphostin AG879, providing further support that Tyrphostin AG879 acts on a distinct signalling pathway to the other three chemicals.

Half of the DEGs identified in Tyrphostin AG879-treated seedlings have been reported as DEGs in a *sesqiα2* SnRK1 hypomorphic mutant (Peixoto *et al.*, 2021). We therefore tested whether Tyrphostin AG879 affects expression of an SnRK1 transcriptional marker, *DARK INDUCIBLE 6* (*DIN6*). Treatment of *DIN6p:LUC* seedlings at dusk with DPI, PI or AEG3482 either had no effect, or slightly inhibited luciferase luminescence, whereas Tyrphostin AG879 increased reporter activity (Fig. S9c). This suggests that Tyrphostin AG879 can activate SnRK1 activity, either directly or indirectly, which is consistent with the increased expression of SnRK1-regulated markers in Tyrphostin AG879-treated seedlings (Fig. S9b). Activation of the starvation response triggered by SnRK1 could explain how Tyrphostin AG879 counteracted the inhibition of seedling growth by DPI (Fig. 4b).

To explore the effect of these four chemicals on primary metabolism, we performed metabolite profiling over a 24 h time-course following treatment with each chemical (Table S4). PCA of 63 metabolites over eight time-points revealed a similar trend

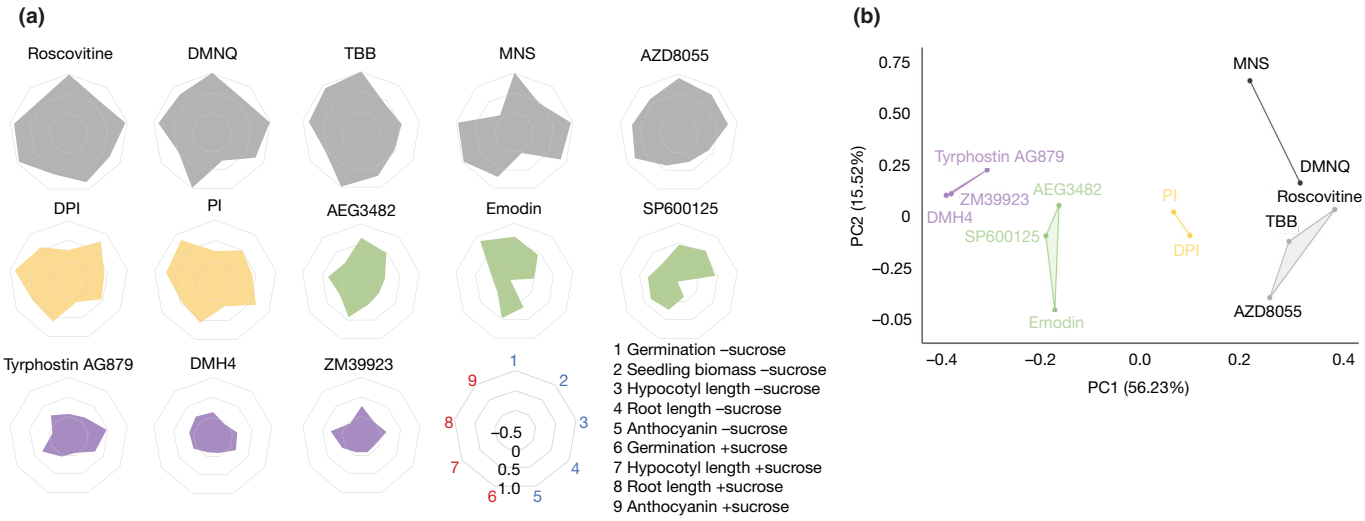

Fig. 4 Summary of effects of LOPAC chemicals on sugar-related growth phenotypes. (a) Normalized effects of the minimum effective concentration of 13 LOPAC chemicals in Arabidopsis compared to DMSO-treated controls on germination of dormant seeds on 30 mM mannitol (1) or sucrose (6), biomass of 7-d-old seedlings on ½MS (2), hypocotyl and root length of 7-d-old dark-grown seedlings on 30 mM mannitol (3, 4) or sucrose (7, 8) and anthocyanin content in 9-d-old seedlings grown for 2 d on 90 mM mannitol (5) or sucrose (9). Charts are arranged in rank order of the sum of normalized effects. Complete data are shown in Supporting Information Figs S4 and S5. (b) *k*-means clustering of growth phenotypes represented in (a). Colours in (a) match clusters in (b).

for all four chemicals in the direction of change compared to DMSO-treated samples for PC1 and PC2, which together explained between 63% and 70% of the variance (Fig. S10). The PC plot for Tyrphostin AG879 suggested a more pronounced effect on the primary metabolome around dusk, compared to the other three chemicals, and the effect of DPI appeared more pronounced than PI and AEG3482.

All four chemicals caused a significant increase in the levels of sucrose, fructose and glucose at more than one time-point. Sucrose was elevated around dawn and glucose and fructose elevated during the day (Fig. 5a). The glycolysis intermediate glucose-6-phosphate was significantly lower in Tyrphostin AG879-treated seedlings at ZT10 and ZT12 and also reduced at ZT24 in seedlings treated with DPI and PI (Fig. 5b). We observed significant increases in tricarboxylic acid (TCA) cycle intermediates, particularly citrate and malate, with the magnitude of the effect increasing with time for all four chemicals (Fig. 5c). Branched-chain amino acids valine, leucine and isoleucine have been associated with HXK1 (Ganpudi *et al.*, 2019) and TOR signalling (Cao *et al.*, 2019) but we did not detect notable changes for any chemical (Fig. 5d). The difference between Tyrphostin AG879 and the other three chemicals detected around dusk in the PCA is probably explained by significantly reduced levels of amino acids at ZT10.5, particularly methionine, threonine and lysine (Fig. 5e), which are all synthesized from oxaloacetate in the TCA cycle.

We have previously shown that DPI inhibits accumulation of superoxide in dark-adapted seedlings treated with sucrose and affects expression of circadian gene expression (Román *et al.*, 2021). The similar phenotypic patterns between DPI and PI suggest they might affect the same sugar signalling pathway. We measured the effect of DPI and PI on circadian rhythms using luciferase reporters and observed lengthening of the circadian period by both chemicals (Fig. 6a,b). This effect is consistent with expectations for inhibition of sugar signalling into the clock, similar to effects of inhibiting sugar production from photosynthesis (Haydon *et al.*, 2013). This effect operates by a SnRK1-dependent mechanism acting on *PRR7* (Frank *et al.*, 2018). However, unlike the effect of the photosystem II inhibitor, 3-(3,4-dichlorophenyl)-1,1-dimethylurea (DCMU), PI or DPI did not elevate *PRR7p:LUC* activity (Fig. 6a). Furthermore, PI or DPI did not inhibit the shortening of circadian period by sucrose in continuous low light (Fig. S11). These suggest the effect of PI and DPI on the circadian period is distinct from the SnRK1-*PRR7* pathway.

The mode of action of PI is not known, but has been reported as an antagonist of both *N*-methyl-D-aspartate (NMDA) glutamate receptors and calmodulin in mammalian cells (Reynolds & Aizenman, 1992; Kitamura *et al.*, 1995). To test if PI similarly affects Ca^{2+} signalling in Arabidopsis we measured the effect of PI on *35Sp:AEQ*, a luminescent reporter for cytosolic Ca^{2+} concentration. We observed rapidly elevated cytosolic Ca^{2+} in PI-treated Arabidopsis seedlings (Fig. 7a), which is inconsistent with PI being a Ca^{2+} channel antagonist but is similar to reported effects of calmodulin inhibitors (Kaplan *et al.*, 2006). We found that two calmodulin inhibitors, W-7 and trifluoperazine (TFP), mimicked effects of PI on circadian gene expression and growth. They both effectively inhibited the transcriptional response to sucrose (Fig. 7b,c), had similar, nonadditive effects on seedling biomass (Fig. 7d) and lengthened the circadian period (Fig. 7e). The elevated cytosolic Ca^{2+} induced by PI or W-7 was prevented by pretreatment with $GaCl_3$, a nonspecific Ca^{2+} channel blocker, but not by DNQX, a GLUTAMATE-LIKE RECEPTOR (GLR) inhibitor (Fig. 7f). These suggest PI is a calmodulin inhibitor that affects GLR-independent Ca^{2+} flux across the plasma membrane.

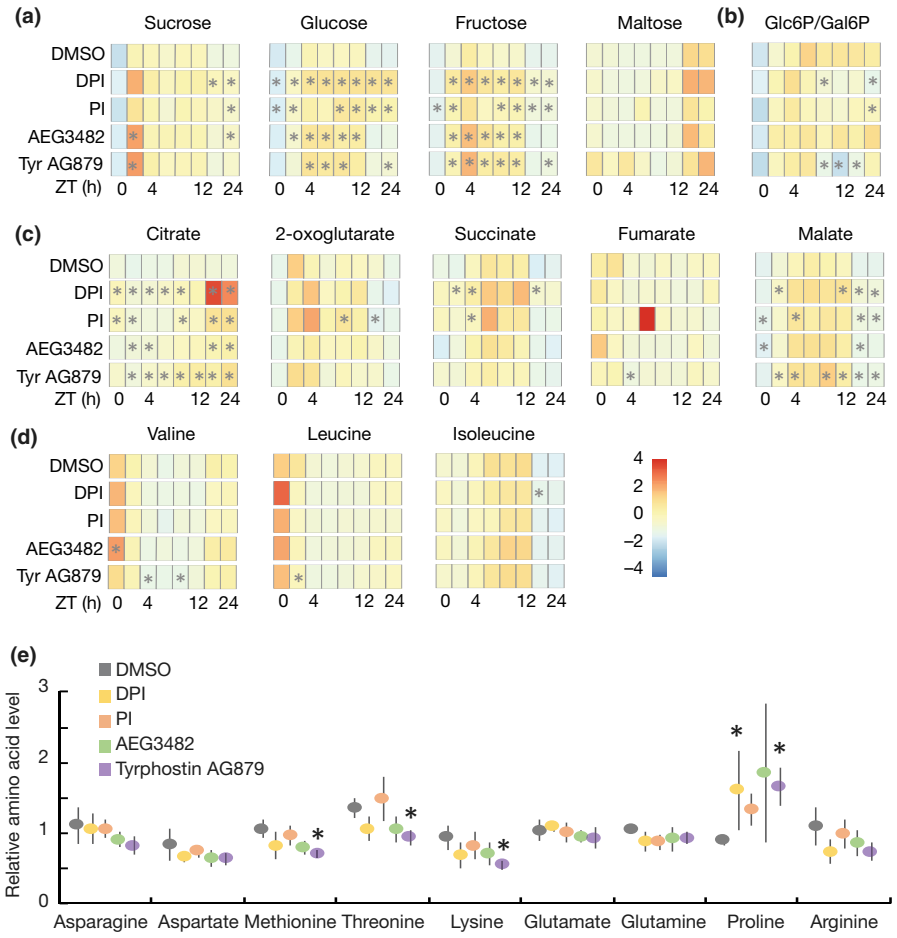

Fig. 5 Primary metabolite levels in chemical-treated Arabidopsis seedlings. (a–d) Heatmaps of relative metabolite levels in seedlings treated with DMSO or chemicals at ZT23 and sampled at ZT0, ZT1.5, ZT4, ZT8, ZT10.5, ZT12, ZT22.5 and ZT24 ($n = 5$; *, $P < 0.05$ compared to DMSO, *t*-test). (e) Relative amino acid levels in DMSO- or chemical-treated seedlings at ZT10.5 (mean ± SD, $n = 5$; *, $P < 0.01$ compared to DMSO, *t*-test).

Since PI strongly affects cytosolic Ca^{2+} concentration and inhibits the transcriptional response to sucrose, we tested whether sucrose could induce a change in cytosolic Ca^{2+} concentration in dark-adapted seedlings. Application of sucrose to dark-adapted seedlings elevated 35Sp:AEQ luminescence compared to mannitol (Fig. 8a). This response was slower than elevation of superoxide observed in sucrose-treated seedlings (Román *et al.*, 2021). Elevation of cytosolic Ca^{2+} concentration by sucrose was attenuated in DPI-treated seedlings. Similarly, although 35Sp:AEQ luminescence was higher in PI-treated seedlings, there was no difference between sucrose and mannitol (Fig. 8a). This is consistent with the targets of these chemicals acting in the same sugar-activated Ca^{2+}-dependent signalling pathway and suggests that the target of DPI acts upstream of the target of PI.

To test whether PI inhibits elevation of superoxide by sucrose, we measured L-012 luminescence and performed NBT stains for superoxide in dark-adapted seedlings. DPI strongly inhibited L-012 luminescence in sucrose-treated seedlings, but PI did not (Fig. 8b). Similarly, NBT stains indicated that, unlike DPI, PI did not prevent sucrose-activated superoxide accumulation (Fig. 8c). These data indicate that the target of PI acts downstream of the target of DPI. This supports the results of the 35Sp:AEQ experiments and suggests that PI might alter the function of an ROS-activated Ca^{2+}-channel acting downstream of NADPH oxidases in a sugar signalling pathway that regulates circadian gene expression.

Discussion

We have used a chemical screen for modifiers of an effect of sucrose on the circadian clock to identify novel experimental tools to manipulate sugar signalling in Arabidopsis. From 75 hit molecules, we confirmed the effect of 13 chemicals and completed broad characterisation of the effects of these chemicals on key sugar-regulated processes including germination, growth and pigmentation. These experiments captured a broad picture of the patterns of phenotypic effects of these chemicals to identify potential shared relationships between them. We selected four chemicals for metabolite and transcriptome profiling, which suggested they affect at least two distinct pathways. Two compounds, DPI and PI, appear to act on a sucrose-activated ROS-Ca^{2+} signalling pathway, which might represent a novel metabolic signalling pathway in Arabidopsis affecting circadian gene expression and growth. Furthermore, this list of commercially available sugar signalling modifiers provides a community resource that could be used to fill gaps in known and unknown metabolic signalling processes in plants, or for other researchers using LOPAC for chemical screens in plant cells.

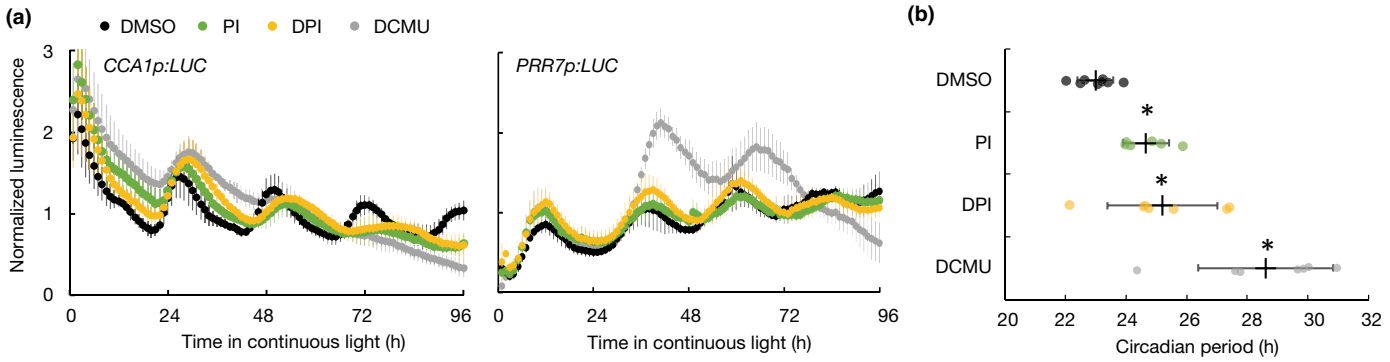

Fig. 6 Effect of pentamidine isethionate (PI) and diphenyleneiodinium (DPI) on the circadian period. (a) Normalized luciferase luminescence in *CCA1p:LUC* and *PRR7p:LUC* Arabidopsis seedlings in continuous light after transfer to media containing DMSO, 25 μM PI, 5 μM DPI or 25 μM DCMU (means ± SD, $n = 4$). (b) Circadian period of luminescence rhythms in *CCA1p:LUC* and *PRR7p:LUC* Arabidopsis seedlings in continuous light (means ± SD, $n = 8$; *, $P < 0.05$ compared to DMSO, Bonferroni-corrected *t*-test).

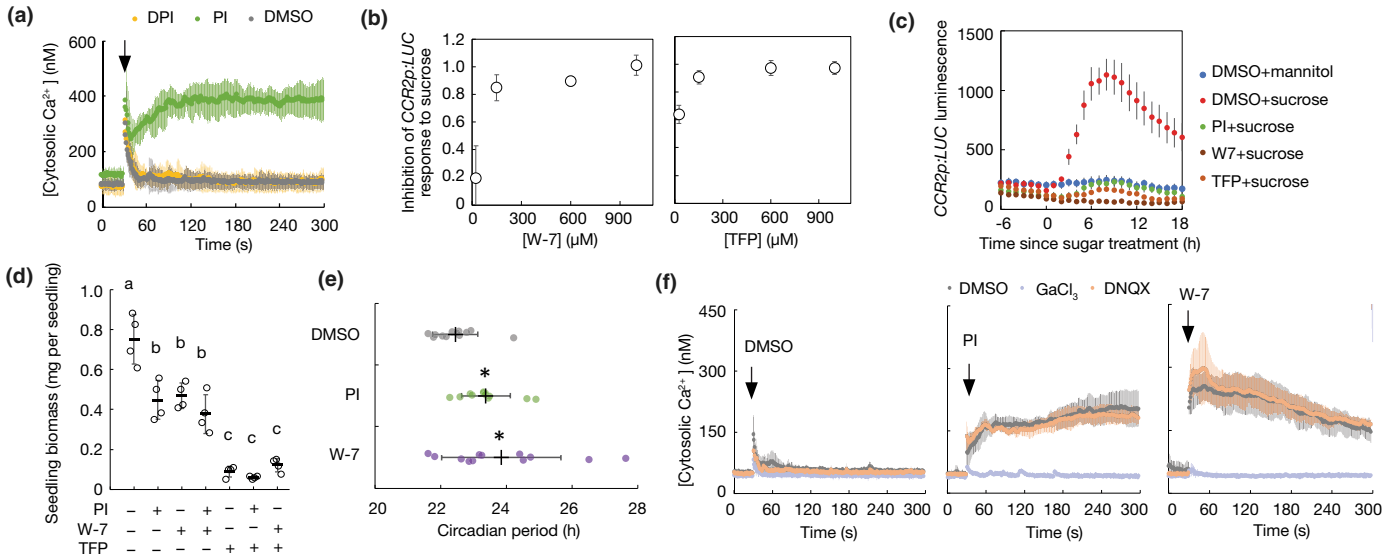

Fig. 7 Pentamidine isethionate (PI) acts like calmodulin inhibitors to elevate cytosolic Ca^{2+}. (a) Cytosolic Ca^{2+} concentration in *35Sp:AEQ* Arabidopsis seedlings treated (arrow) with DMSO (control), 10 μM diphenyleneiodinium (DPI) or 25 μM PI (means ± SD, $n = 6$). (b) Inhibition of peak luciferase luminescence in dark-adapted *CCR2p:LUC* Arabidopsis seedlings after treatment with 30 mM sucrose in the presence of the indicated concentration of chemical compared to DMSO-treated controls (means ± SEM, $n = 8$). (c) Luciferase luminescence in dark-adapted *CCR2p:LUC* Arabidopsis seedlings treated with 30 mM mannitol or 30 mM sucrose in the presence of DMSO (control), 25 μM PI, 150 μM W-7 or 150 μM trifluoperazine (TFP) (means ± SEM, $n = 8$). (d) Seedling biomass of 7-d-old Arabidopsis Col-0 seedlings sown on combinations of DMSO, 5 μM PI, 25 μM W-7 and 25 μM TFP (means ± SD, $n = 4$ of 12 seedlings; different letters indicate $P < 0.01$, one-way ANOVA with Tukey's HSD). (e) Circadian period estimates of luciferase luminescence in *PRR7p:LUC*, *CCR2p:LUC* and *TOC1p:LUC* Arabidopsis seedlings in continuous light treated with DMSO (control), 25 μM PI or 150 μM W-7 (means ± SD, $n = 12$; *, $P < 0.05$ compared to DMSO, Bonferroni-corrected *t*-test). (f) Cytosolic Ca^{2+} concentration in *35Sp:AEQ* Arabidopsis seedlings treated with DMSO (control), 100 μM PI or 150 μM W-7 in the presence of DMSO (control), 1 mM $GaCl_3$ or 1 mM DNQX (means ± SD, $n = 4$).

The effect of Tyrphostin AG879 on the transcriptome suggested that it might be a modifier of SnRK1 or a SnRK1-related pathway and we confirmed that this chemical could activate *DIN6p:LUC*, a reporter of SnRK1 activity. Although the number of DEGs was small in Tyrphostin AG879-treated seedlings around dawn, this is consistent with the small effect of *SnRK1α*-overexpression on the transcriptome and the apparently higher activity of SnRK1 at this time of day (Peixoto *et al.*, 2021). A SnRK1 activator could be expected to inhibit the transcriptional response of *CCR2p:LUC* to sucrose in C-starved seedlings. Two other chemicals, DMH4 and ZM39923, which are also annotated as tyrosine kinase inhibitors, had similar patterns of effects to Tyrphostin AG879, so it is possible that these also influence SnRK1-related signalling.

The TOR kinase inhibitor, AZD8055, is not represented in LOPAC but was included in our experiments because we found it was able to inhibit the transcriptional response to sucrose. Although the effect on the luciferase reporter was relatively weak, the effect on the transcript was strong. TOR is activated by sugar availability and influences circadian rhythms in Arabidopsis (Zhang *et al.*, 2019), so it is possible other modifiers of plant TOR signalling could have been identified in our screen. Based

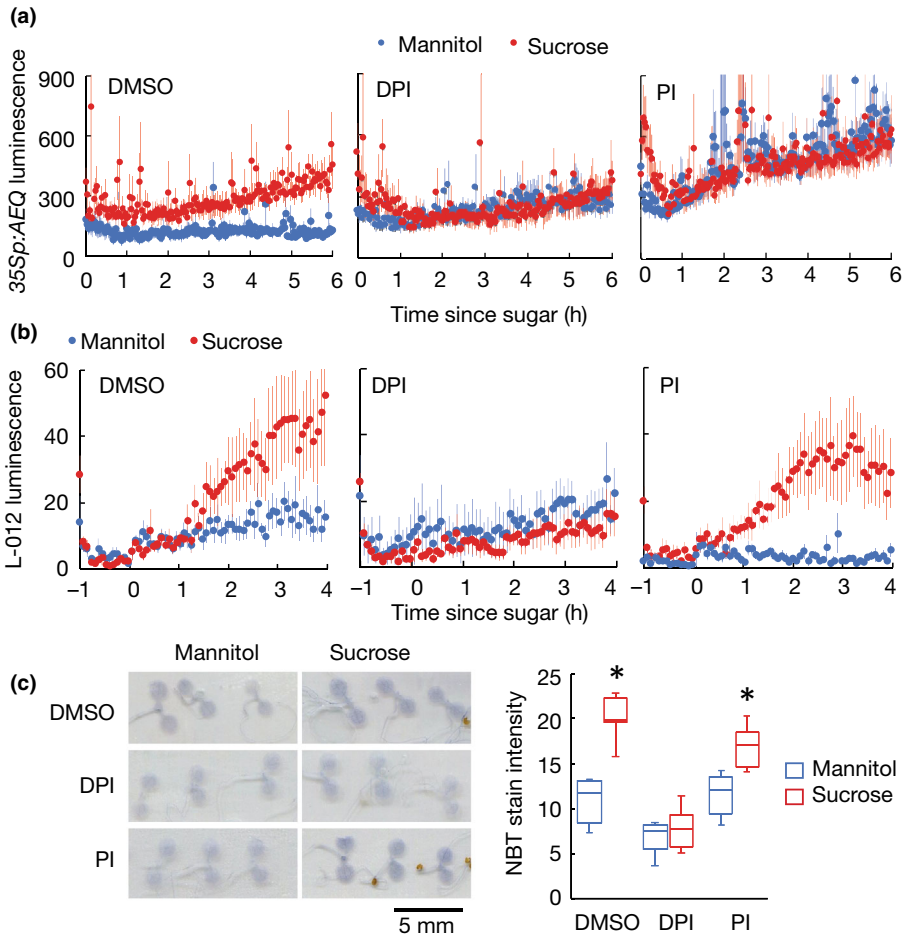

Fig. 8 Pentamidine isethionate (PI) acts downstream of diphenyleneiodinium (DPI). (a) Aequorin luminescence in dark-adapted *35Sp:AEQ* Arabidopsis seedlings treated with 30 mM sucrose or mannitol in the presence of DMSO, 5 μM DPI or 25 μM PI (mean ± SD, $n = 6$). (b) L-012 luminescence in dark-adapted Arabidopsis Col-0 seedlings treated with 30 mM mannitol or sucrose in the presence of DMSO, 10 μM DPI or 25 μM PI (means ± SEM, $n = 6$). (c) Images and quantification of nitroblue tetrazolium (NBT) stain for superoxide in dark-adapted Arabidopsis Col-0 seedlings 4 h after treatment with 30 mM mannitol or sucrose in the presence of DMSO, 5 μM DPI or 25 μM PI (Tukey boxplots, $n = 8$; *, $P < 0.05$ compared to mannitol, Bonferroni-corrected *t*-test).

on phenotypic effects, the most similar chemicals were roscovitine, a cyclin-dependent kinase inhibitor, and TBB. Although TBB is a CK2 inhibitor, it appears this is not the mechanism by which it affects expression of *CCR2* in our experiments.

Diphenyleneiodinium and pentamidine isethionate have very similar effects on the phenotypes we measured and their inhibition of growth is not additive, suggesting they act on the same pathway. DPI inhibits accumulation of superoxide in sucrose-treated seedlings, probably by inhibiting NADPH oxidases at the plasma membrane because other NADPH oxidase inhibitors have similar effects (Román *et al.*, 2021). PI is likely to act as a calmodulin inhibitor that controls movement of Ca^{2+} across the plasma membrane. Calmodulin (CaM) and CaM-LIKE (CML) proteins have various regulatory functions but can inhibit Ca^{2+} channels or activate Ca^{2+} pumps (Astegno *et al.*, 2017; Tian *et al.*, 2020). CML proteins have been implicated in sugar responses and circadian rhythms (Bender *et al.*, 2013; Martí Ruiz *et al.*, 2018). Consistent with a role for Ca^{2+} signalling in the transcriptional sugar response, application of sucrose to dark-adapted seedlings elevated cytosolic Ca^{2+}, with a slightly slower response than the accumulation of superoxide. Since PI did not inhibit sucrose-activated superoxide accumulation, the Ca^{2+} signal seems to act downstream of the superoxide signal and PI might affect activity of an ROS-activated Ca^{2+}channel. CYCLIC NUCLEOTIDE GATED Ca^{2+} CHANNELs (CNGCs) and ANNEXINs have been proposed to fulfil this role in plants (Demidchik, 2018). By contrast, GLRs have been shown to act upstream of NADPH oxidases (Kong *et al.*, 2016) and our data suggest that PI-stimulated Ca^{2+} influx is not via GLRs since it is unaffected by a GLR inhibitor, DNQX. Nevertheless, all these channels are members of large protein families, so genetic verification to implicate or exclude any of these proteins will be challenging.

If our results suggest a novel sugar signalling pathway, a critical question is how the sugar is sensed. Since NADPH oxidases are present on the plasma membrane, this could be an extracellular sugar-sensing mechanism. A role for RGS1 seems unlikely since G-protein mutants are not affected in the sucrose response assay. Receptor-like kinases have been implicated in numerous extracellular signalling pathways, upstream of NADPH oxidases. This is a very large protein family, but many of these contain sugar-binding lectin domains (Sun *et al.*, 2020). However, NADPH oxidases can be triggered by intracellular domains, so it is also possible that sugars are sensed within cells. Alternatively, DPI might be inhibiting superoxide accumulation in a different location. It will be important to determine the cellular location of both the superoxide accumulation and Ca^{2+} signal in the future.

Confirming the direct targets of these chemicals will be important to define these signalling pathways. A forward genetics approach lacks sufficient specificity and the likelihood of isolating loss-of-function mutations in essential sugar signalling proteins

will be small, since these are expected to be lethal. Reverse genetics is limited when there is functional redundancy within protein families. Therefore, chemical proteomics has the most promise (Hicks & Raikhel, 2014), although these techniques can be particularly challenging for membrane proteins. Nevertheless, this chemical screen has successfully identified a new set of pharmacological tools to manipulate sugar signalling and circadian rhythms in plant cells. This provides the opportunity to discover new signalling pathways in Arabidopsis and it will be informative to test the efficacy of these chemicals in other plant species.

Acknowledgements

We thank Waheed Arshad and Heather Eastmond for technical assistance, Heather McFarlane and Antony Dodd for sharing seeds, and Mark Greenwood for advice on luminescence camera configuration. This research was funded by a Royal Society Research Grant (RG150144), the Botany Foundation, a Thomas Davies Research Grant from the Australian Academy of Science and the University of Melbourne through the Research Grants Support Scheme to MJH and Melbourne Research Scholarships to XL and GC. Open access publishing facilitated by The University of Melbourne, as part of the Wiley - The University of Melbourne agreement via the Council of Australian University Librarians.

Author contributions

MJH conceived the study; XL, DD, GC, AR, CRB, CCM-B, AS, CC and MJH designed experiments and analysed the data; XL, DD, GC, AR, CCM-B and MJH performed experiments; XL and MJH wrote the manuscript; all authors edited and approved the manuscript.

ORCID

Christopher R. Buckley https://orcid.org/0000-0002-4095-2300
Camila Caldana https://orcid.org/0000-0003-3639-0621
Michael J. Haydon https://orcid.org/0000-0003-2486-9387
Xiang Li https://orcid.org/0000-0002-6325-6439
Ángela Román https://orcid.org/0000-0003-3457-999X
Aleksandra Skirycz https://orcid.org/0000-0002-7627-7925

Data availability

Raw sequencing files and processed data for RNA-seq have been deposited in the NCBI Gene Expression Omnibus (GSE188596).

References

Astegno A, Bonza MC, Vallone R, la Verde V, D'Onofrio M, Luoni L, Molesini B, Dominici P. 2017. Arabidopsis calmodulin-like protein CML36 is a calcium (Ca^{2+}) sensor that interacts with the plasma membrane Ca^{2+}-ATPase isoform ACA8 and stimulates its activity. *Journal of Biological Chemistry* **292**: 15049–15061.

Baena-González E, Rolland F, Thevelein JM, Sheen J. 2007. A central integrator of transcription networks in plant stress and energy signalling. *Nature* **448**: 938–942.

Belda-Palazón B, Adamo M, Valerio C, Ferreira LJ, Confraria A, Reis-Barata D, Rodrigues A, Meyer C, Rodriguez PL, Baena-González E. 2020. A dual function of SnRK2 kinases in the regulation of SnRK1 and plant growth. *Nature Plants* **6**: 1345–1353.

Bender KW, Rosenbaum DM, Vanderbeld B, Ubaid M, Snedden WA. 2013. The Arabidopsis calmodulin-like protein, CML39, functions during early seedling establishment. *The Plant Journal* **76**: 634–647.

Burkart GM, Brandizzi F. 2021. A tour of TOR complex signaling in plants. *Trends in Biochemical Sciences* **46**: 417–428.

Cao P, Kim SJ, Xing A, Schenck CA, Liu L, Jiang N, Wang J, Last RL, Brandizzi F. 2019. Homeostasis of branched-chain amino acids is critical for the activity of TOR signaling in Arabidopsis. *eLife* **8**: e50747.

Chen J-G, Willard FS, Huang J, Liang J, Chasse SA, Jones AM, Siderovski DP. 2003. A seven-transmembrane RGS protein that modulates plant cell proliferation. *Science* **301**: 1728–1731.

Chen Q, Xu X, Xu D, Zhang H, Zhang C, Li G. 2019. WRKY18 and WRKY53 coordinate with HISTONE ACETYLTRANSFERASE1 to regulate rapid responses to sugar. *Plant Physiology* **180**: 2212–2226.

Chen Y, Chen Y, Shi C, Huang Z, Zhang Y, Li S, Li Y, Ye J, Yu C, Li Z *et al.* 2018. SOAPNUKE: a MapReduce acceleration-supported software for integrated quality control and preprocessing of high-throughput sequencing data. *GigaScience* **7**: 1–6.

Chen Y, Ji F, Xie H, Liang J, Zhang J. 2006. The regulator of G-protein signaling proteins involved in sugar and abscisic acid signaling in Arabidopsis seed germination. *Plant Physiology* **140**: 302–310.

Cho YH, Yoo SD, Sheen J. 2006. Regulatory functions of nuclear Hexokinase1 complex in glucose signaling. *Cell* **127**: 579–589.

Cuadros-Inostroza Á, Caldana C, Redestig H, Kusano M, Lisec J, Peña-Cortés H, Willmitzer L, Hannah MA. 2009. TARGETSEARCH – a BIOCONDUCTOR package for the efficient preprocessing of GC-MS metabolite profiling data. *BMC Bioinformatics* **10**: 428.

Dalchau N, Baek SJ, Briggs HM, Robertson FC, Dodd AN, Gardner MJ, Stancombe MA, Haydon MJ, Stan G-B, Gonçalves JM *et al.* 2011. The circadian oscillator gene *GIGANTEA* mediates a long-term response of the *Arabidopsis thaliana* circadian clock to sucrose. *Proceedings of the National Academy of Sciences, USA* **108**: 5104–5109.

Dalchau N, Hubbard KE, Robertson FC, Hotta CT, Briggs HM, Stan G-B, Gonçalves JM, Webb AAR. 2010. Correct biological timing in Arabidopsis requires multiple light-signaling pathways. *Proceedings of the National Academy of Sciences, USA* **107**: 13171–13176.

Demidchik V. 2018. ROS-activated ion channels in plants: biophysical characteristics, physiological functions and molecular nature. *International Journal of Molecular Sciences* **19**: 1263.

Doyle MR, Davis SJ, Bastow RM, McWatters HG, Kozma-Bognár L, Nagy F, Millar AJ, Amasino RM. 2002. The *ELF4* gene controls circadian rhythms and flowering time in *Arabidopsis thaliana*. *Nature* **419**: 74–77.

Eastmond PJ, van Dijken AJH, Spielman M, Kerr A, Tissier AF, Dickinson HG, Jones JDG, Smeekens SC, Graham IA. 2002. Trehalose-6-phosphate synthase 1, which catalyses the first step in trehalose synthesis, is essential for Arabidopsis embryo maturation. *The Plant Journal* **29**: 225–235.

Figueroa CM, Lunn JE. 2016. A tale of two sugars: trehalose 6-phosphate and sucrose. *Plant Physiology* **172**: 7–27.

Frank A, Matiolli CC, Viana JC, Vincentz M, Webb AAR, Dodd AN, Viana JC, Hearn TJ, Kusakina J. 2018. Circadian entrainment in Arabidopsis by the sugar-responsive transcription factor bZIP63. *Current Biology* **28**: 2597–2606.

Fricker MD, Plieth C, Knight H, Blancaflor E, Knight MR, White NS, Gilroy S. 1999. Fluorescence and luminescence techniques to probe ion activities in living plant cells. In: Mason WT, ed. *Fluorescent and luminescent probes for biological activity: a practical guide to technology for quantitative real-time analysis*. Cambridge, MA, USA: Elsevier, 569–596.

Ganpudi A, Romanowski A, Halliday KJ. 2019. HEXOKINASE 1 glycolytic action fuels post-germinative seedling growth. *bioRxiv*. doi: 10.1101/548990.

Giavalisco P, Li Y, Matthes A, Eckhardt A, Hubberten HM, Hesse H, Segu S, Hummel J, Köhl K, Willmitzer L. 2011. Elemental formula annotation of

polar and lipophilic metabolites using ^{13}C, ^{15}N and ^{34}S isotope labelling, in combination with high-resolution mass spectrometry. *The Plant Journal* **68**: 364–376.

Gómez LD, Gilday A, Feil R, Lunn JE, Graham IA. 2010. AtTPS1-mediated trehalose 6-phosphate synthesis is essential for embryogenic and vegetative growth and responsiveness to ABA in germinating seeds and stomatal guard cells. *The Plant Journal* **64**: 1–13.

Haydon MJ, Kawachi M, Wirtz M, Hillmer S, Hell R, Krämer U. 2012. Vacuolar nicotianamine has critical and distinct roles under iron deficiency and for zinc sequestration in Arabidopsis. *Plant Cell* **24**: 724–737.

Haydon MJ, Mielczarek O, Frank A, Román Á, Webb AAR. 2017. Sucrose and ethylene signaling interact to modulate the circadian clock. *Plant Physiology* **175**: 947–958.

Haydon MJ, Mielczarek O, Robertson FC, Hubbard KE, Webb AAR. 2013. Photosynthetic entrainment of the *Arabidopsis thaliana* circadian clock. *Nature* **502**: 689–692.

Hicks GR, Raikhel NV. 2014. Plant chemical biology: are we meeting the promise? *Frontiers in Plant Science* **5**: 455.

Huang JP, Tunc-Ozdemir M, Chang Y, Jones AM. 2015. Cooperative control between AtRGS1 and AtHXK1 in a WD40-repeat protein pathway in *Arabidopsis thaliana*. *Frontiers in Plant Science* **6**: 851.

Huege J, Krall L, Steinhauser MC, Giavalisco P, Rippka R, Tandeau De Marsac N, Steinhauser D. 2011. Sample amount alternatives for data adjustment in comparative cyanobacterial metabolomics. *Analytical and Bioanalytical Chemistry* **399**: 3503–3517.

Jones AM, Ecker JR, Chen JG. 2003. A reevaluation of the role of the heterotrimeric G protein in coupling light responses in Arabidopsis. *Plant Physiology* **131**: 1623–1627.

Kaplan B, Davydov O, Knight H, Galon Y, Knight MR, Fluhr R, Fromm H. 2006. Rapid transcriptome changes induced by cytosolic Ca^{2+} transients reveal ABRE-related sequences as Ca^{2+}-responsive *cis* elements in *Arabidopsis*. *Plant Cell* **18**: 2733–2748.

Kim D, Langmead B, Salzberg SL. 2015. HISAT: a fast spliced aligner with low memory requirements. *Nature Methods* **12**: 357–360.

Kitamura Y, Arima T, Imaizumi R, Sato T, Nomura Y. 1995. Inhibition of constitutive nitric oxide synthase in the brain by pentamidine, a calmodulin antagonist. *European Journal of Pharmacology: Molecular Pharmacology* **289**: 299–304.

Kong D, Hu H-C, Okuma E, Lee Y, Lee HS, Munemasa S, Cho D, Ju C, Pedoeim L, Rodrigues B *et al.* 2016. L-Met activates Arabidopsis GLR Ca^{2+} channels upstream of ROS production and regulates stomatal movement. *Cell Reports* **17**: 2553–2561.

Li B, Dewey CN. 2011. RSEM: accurate transcript quantification from RNA-Seq data with or without a reference genome. *BMC Bioinformatics* **12**: 323.

List M, Schmidt S, Christiansen H, Rehmsmeier M, Tan Q, Mollenhauer J, Baumbach J. 2016. Comprehensive analysis of high-throughput screens with HITSEEKR. *Nucleic Acids Research* **44**: 6639–6648.

Liu W, Feke A, Leung CC, Tarté DA, Yuan W, Vanderwall M, Sager G, Wu X, Schear A, Clark DA *et al.* 2021. A metabolic daylength measurement system mediates winter photoperiodism in plants. *Developmental Cell* **56**: 2501–2515.e5.

Mair A, Pedrotti L, Wurzinger B, Anrather D, Simeunovic A, Weiste C, Valerio C, Dietrich K, Kirchler T, Nägele T *et al.* 2015. SnRK1-triggered switch of bZIP63 dimerization mediates the low-energy response in plants. *eLife* **4**: 1–33.

Martí Ruiz MC, Hubbard KE, Gardner MJ, Jung HJ, Aubry S, Hotta CT, Mohd-noh NI, Robertson FC, Hearn TJ, Tsai Y *et al.* 2018. Circadian oscillations of cytosolic free calcium regulate the Arabidopsis circadian clock. *Nature Plants* **4**: 690–698.

Menand B, Desnos T, Nussaume L, Berger F, Bouchez D, Meyer C, Robaglia C. 2002. Expression and disruption of the Arabidopsis TOR (target of rapamycin) gene. *Proceedings of the National Academy of Sciences, USA* **99**: 6422–6427.

Montané MH, Menand B. 2013. ATP-competitive mTOR kinase inhibitors delay plant growth by triggering early differentiation of meristematic cells but no developmental patterning change. *Journal of Experimental Botany* **64**: 4361–4374.

Moore B, Zhou L, Rolland F, Hall Q, Cheng W-H, Liu Y-X, Hwang I, Jones T, Sheen J. 2003. Role of the Arabidopsis glucose sensor HXK1 in nutrient, light, and hormonal signaling. *Science* **300**: 332–336.

Nakamichi N, Kita M, Ito S, Yamashino T, Mizuno T. 2005. PSEUDO-RESPONSE REGULATORS, PRR9, PRR7 and PRR5, together play essential roles close to the circadian clock of *Arabidopsis thaliana*. *Plant and Cell Physiology* **46**: 686–698.

Peixoto B, Moraes TA, Mengin V, Margalha L, Vicente R, Feil R, Höhne M, Sousa AGG, Lilue J, Stitt M *et al.* 2021. Impact of the SnRK1 protein kinase on sucrose homeostasis and the transcriptome during the diel cycle. *Plant Physiology* **187**: 1357–1373.

Porra RJ. 1989. Determination of accurate extinction coefficients and simultaneous equations for assaying chlorophylls a and b extracted with four different solvents: verification of the concentration of chlorophyll standards by atomic absorption spectroscopy. *Biochimica et Biophysica Acta* **975**: 384–394.

Portolés S, Más P. 2010. The functional interplay between protein kinase CK2 and cca1 transcriptional activity is essential for clock temperature compensation in Arabidopsis. *PLoS Genetics* **6**: e1001201.

R Core Team. 2021. *R: a language and environment for statistical computing*. Vienna, Austria: R Foundation for Statistical Computing.

Ramon M, Dang TVT, Broeckx T, Hulsmans S, Crepin N, Sheen J, Rolland F. 2019. Default activation and nuclear translocation of the plant cellular energy sensor SnRK1 regulate metabolic stress responses and development. *Plant Cell* **31**: 1614–1632.

Reynolds I, Aizenman E. 1992. Pentamidine is an N-methyl-D-aspartate receptor antagonist and is neuroprotective *in vitro*. *Journal of Neuroscience* **12**: 970–975.

Roessner U, Luedemann A, Brust D, Fiehn O, Linke T, Willmitzer L, Fernie AR. 2001. Metabolic profiling allows comprehensive phenotyping of genetically or environmentally modified plant systems. *Plant Cell* **13**: 11–29.

Rolland F, Baena-Gonzalez E, Sheen J. 2006. Sugar sensing and signaling in plants: conserved and novel mechanisms. *Annual Review of Plant Biology* **57**: 675–709.

Román Á, Li X, Deng D, Davey JW, James S, Graham IA, Haydon MJ. 2021. Superoxide is promoted by sucrose and affects amplitude of circadian rhythms in the evening. *Proceedings of the National Academy of Sciences, USA* **118**: e2020646118.

Ruijter JM, Ramakers C, Hoogaars WMH, Karlen Y, Bakker O, van den Hoff MJB, Moorman AFM. 2009. Amplification efficiency: linking baseline and bias in the analysis of quantitative PCR data. *Nucleic Acids Research* **37**: e45.

Segarra S, Mir R, Martínez C, León J. 2010. Genome-wide analyses of the transcriptomes of salicylic acid-deficient versus wild-type plants uncover pathogen and circadian controlled 1 (PCC1) as a regulator of flowering time in Arabidopsis. *Plant, Cell & Environment* **33**: 11–22.

Stacklies W, Redestig H, Scholz M, Walther D, Selbig J. 2007. PCAMETHODS – a BIOCONDUCTOR package providing PCA methods for incomplete data. *Bioinformatics* **23**: 1164–1167.

Sun Y, Qiao Z, Muchero W, Chen J-G. 2020. Lectin receptor-like kinases: the sensor and mediator at the plant cell surface. *Frontiers in Plant Science* **11**: 596301.

Tarazona S, Furió-Tarí P, Turrà D, di Pietro A, Nueda MJ, Ferrer A, Conesa A. 2015. Data quality aware analysis of differential expression in RNA-seq with NOISEQ R/BIOC package. *Nucleic Acids Research* **43**: e140.

Thorne N, Shen M, Lea WA, Simeonov A, Lovell S, Auld DS, Inglese J. 2012. Firefly luciferase in chemical biology: a compendium of inhibitors, mechanistic evaluation of chemotypes, and suggested use as a reporter. *Chemistry and Biology* **19**: 1060–1072.

Thung L, Trusov Y, Chakravorty D, Botella JR. 2012. Gγ1+Gγ2+Gγ3=Gβ: the search for heterotrimeric G-protein γ subunits in Arabidopsis is over. *Journal of Plant Physiology* **169**: 542–545.

Tian W, Wang C, Gao Q, Li L, Luan S. 2020. Calcium spikes, waves and oscillations in plant development and biotic interactions. *Nature Plants* **6**: 750–759.

Ullah H, Chen J, Temple B, Boyes DC, Alonso JM, Davis KR, Ecker JR, Jones AM. 2003. The β-subunit of the Arabidopsis G protein negatively regulates auxin-induced cell division and affects multiple developmental processes. *Plant Cell* **15**: 393–409.

Urano D, Phan N, Jones JC, Yang J, Huang J, Grigston J, Taylor JP, Jones AM. 2012. Endocytosis of the seven-transmembrane RGS1 protein activates G-protein-coupled signalling in Arabidopsis. *Nature Cell Biology* **14**: 1079–1088.

Wang Y, Chang H, Hu S, Lu X, Yuan C, Zhang C, Wang P, Xiao W, Xiao L, Xue G *et al.* 2014. Plastid casein kinase 2 knockout reduces abscisic acid (ABA) sensitivity, thermotolerance, and expression of ABA- and heat-stress-responsive nuclear genes. *Journal of Experimental Botany* **65**: 4159–4175.

Weckwerth W, Ehlers Loureiro M, Wenzel K, Fiehn O. 2004. Differential metabolic networks unravel the effects of silent plant phenotypes. *Proceedings of the National Academy of Sciences, USA* **101**: 7809–7814.

Xiong Y, McCormack M, Li L, Hall Q, Xiang C, Sheen J. 2013. Glucose-TOR signalling reprograms the transcriptome and activates meristems. *Nature* **496**: 181–186.

Zhang N, Meng Y, Li X, Zhou Y, Ma L, Fu L, Schwarzländer M, Liu H, Xiong Y. 2019. Metabolite-mediated TOR signaling regulates the circadian clock in Arabidopsis. *Proceedings of the National Academy of Sciences, USA* **116**: 25395–25397.

Zhang Y, Primavesi LF, Jhurreea D, Andralojc PJ, Mitchell RAC, Powers SJ, Schluepmann H, Delatte T, Wingler A, Paul MJ. 2009. Inhibition of SNF1-related protein kinase1 activity and regulation of metabolic pathways by trehalose-6-phosphate. *Plant Physiology* **149**: 1860–1871.

Supporting Information

Additional Supporting Information may be found online in the Supporting Information section at the end of the article.

Fig. S1 Mg-ATP does not activate *CCR2p:LUC*.

Fig. S2 Inhibition of luciferase luminescence by LOPAC (Library of Pharmacologically Active Compounds) chemicals.

Fig. S3 Structures of 15 chemicals chosen for validation.

Fig. S4 Inhibition of the transcriptional response to sucrose.

Fig. S5 CK2 is not required for *CCR2* response to sucrose.

Fig. S6 Effect of chemicals on germination of dormant seeds.

Fig. S7 Effects of chemicals on growth and pigments.

Fig. S8 Additive and nonadditive effects of chemicals in combination.

Fig. S9 Effect of selected chemicals on transcriptome at dawn.

Fig. S10 Principal component analysis of effects of chemicals on primary metabolites.

Fig. S11 PI and DPI do not inhibit effect of sucrose on period in continuous low light.

Table S1 Primers used in this study.

Table S2 LOPAC (Library of Pharmacologically Active Compounds) chemicals that modify *CCR2p:LUC* reporter response to sucrose, strictly standardized mean difference $\pm$ 1.

Table S3 Differentially expressed genes identified by RNA-sequencing in untreated seedlings or seedlings treated with DMSO, DPI, PI, AEG3482 or Tyrphostin AG879.

Table S4 Metabolite profiling in untreated seedlings or seedlings treated with DMSO, DPI, PI, AEG3482 or Tyrphostin AG879.

Please note: Wiley Blackwell are not responsible for the content or functionality of any Supporting Information supplied by the authors. Any queries (other than missing material) should be directed to the *New Phytologist* Central Office.